Electronic Supporting Information of:

One-Step Synthesis of TiO_2/Graphene Nanocomposites by Laser Pyrolysis with Well-Controlled Properties and Application in Perovskite Solar Cells

Raphaëlle Belchi[1,2], Aurélie Habert[1], Eddy Foy[1], Alexandre Gheno[2], Sylvain Vedraine[2], Rémi Antony[2], Bernard Ratier[2], Johann Bouclé[2,*], Nathalie Herlin-Boime[1,*]

[1] *NIMBE, CEA, CNRS, Université Paris-Saclay, CEA Saclay 91191 Gif-sur-Yvette, France*

[2] *Univ. Limoges, CNRS, XLIM, UMR 7252, F-87000 Limoges, France*

* Corresponding authors: johann.boucle@unilim.fr; nathalie.herlin@cea.fr

Experimental Details

The compact TiO_2 layer is elaborated from a solution of titanium isopropoxide (TTIP, Sigma-Aldrich) in absolute ethanol (15.4 µL/mL). This one is deposited by spin-coating and annealed at 450°C for 20 min. Mesoporous TiO_2 and TiO_2/graphene electron transport layer of our solar cells were elaborated from the nanomaterials synthesised by laser pyrolysis. A solution was prepared with 190 µL of absolute ethanol, 43 µL of α –terpineol and 5 mg of the powder in which 100 mg of a solution of 40 mg ethyl-cellulose with 456 µL absolute ethanol was added. The obtained paste is sonicated for 1 hour and stirred during the night. It is then spin-coated at 4000 rpm for 60 seconds and the sample is annealed progressively up to 430°C to remove all organic components. Both TiO_2 layers are immerged into a bath of 220 µL $TiCl_4$ diluted into 100 mL of distilled water for 30 min at 70°C and annealed again at 450°C and 430°C respectively.

The solar absorber deposited on top of the mesoporous electron transport TiO_2 layer is a $CH_3NH_3PbI_{3-x}Cl_x$ perovskite. The precursor is a solution of 40 wt.% $PbCl_2$ and CH_3NH_3I with a molar ratio of 1:3, 59 wt.% of DMF and 1 wt.% 1,8-diiodooctane. The deposition of the perovskite is made in a single-step using spin-coating under nitrogen flow. The sample is then annealed at 90°C for 2 hours for an optimal crystallization. Further details on the experimental procedure used for device preparation are reported in the literature [1].

The crystalline phases of the materials were identified by X-Ray diffraction analysis (Rigaku Ru200BH) using a molybdenum anode (λ=0.70932 Å). Structural properties were probed by Raman spectroscopy using both a 633 nm red laser (LabRAM HR Evolution – Horiba) and a 532 nm green laser (XploRA PLUS – Horiba).

In addition, steady-state photoluminescence spectra were measured in the 720-850 nm range using FLS980 spectrometer (Edinburg Instruments, UK). The excitation (510 nm) is provided by a monochromated 450W Xenon lamp and the detection operated by a cooled R928P Hamamatsu photomultiplier. Quantitative measurements were obtained by normalizing the emission spectra by the effective fraction of light absorbed at the excitation wavelength, ensuring similar excitation conditions for all samples. Transient PL measurements were performed using the same apparatus equipped with picosecond laser diode emitting at 510 nm with a temporal width of 150 ps and a fast response photodetector. The detection was made through time-correlated single photon counting (TCSPC), and the traces were adjusted by taking into account the instrument response function (IRF), estimated using a diffusive reference sample.

Current density–voltage (J–V) characteristics were recorded in ambient conditions on un-capsulated devices (around 50% of relative humidity and in ambient air). A calibrated Keithley 2400 source-measure unit was used with a solar simulator (1600W NEWPORT) equipped with an AM1.5G filter. The spectral mismatch between the emission of the solar simulator and the global AM1.5G solar spectrum was taken into account using standard procedures (IEC 60904-9 Edition 2) and the solar simulator irradiance was corrected accordingly to match 100 mW cm^{-2} on the tested cell. The cells were masked with an aperture of 0.2 cm^2. Scan rates in the order of 80 $mV.s^{-1}$ were used as they were found to minimize the hysteresis effect in our conditions.

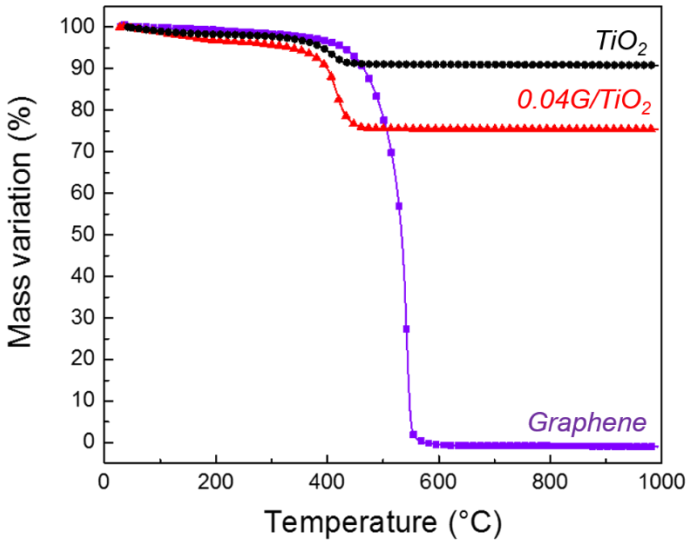

Figure S1 Thermogravimetric Analysis (TGA) of the pristine graphene and the powder obtained after laser pyrolysis: TiO_2 and 0.04G/TiO_2

Thermogravimetric Analysis (TGA) were conducted by heating the powders under air up to 1000°C (10°C/min). Graphene starts to be degraded from 450°C whereas amorphous carbon present in the TiO_2 and 0.04G/TiO_2 powders is eliminated after 400°C (cf. Figure S1). Therefore annealing treatment was fixed at 430°C to remove the undesirable carbon material.

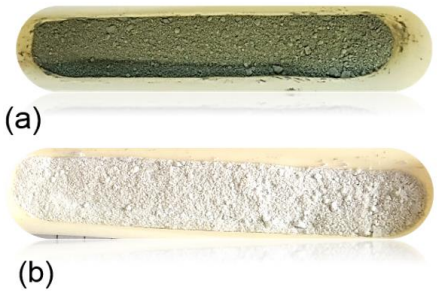

Figure S2 Aspect of a typical TiO_2/graphene nanopowder obtained by laser pyrolysis before (a) and after (b) thermal annealing at 430°C for 6h in air.

The darkened colour of the TiO_2-based powder after laser pyrolysis is due to the presence of the amorphous carbon (Figure S2 (a)). After removal of the carbon by annealing, the white characteristic colour of the TiO_2 is predominant (Figure S2 (b)).

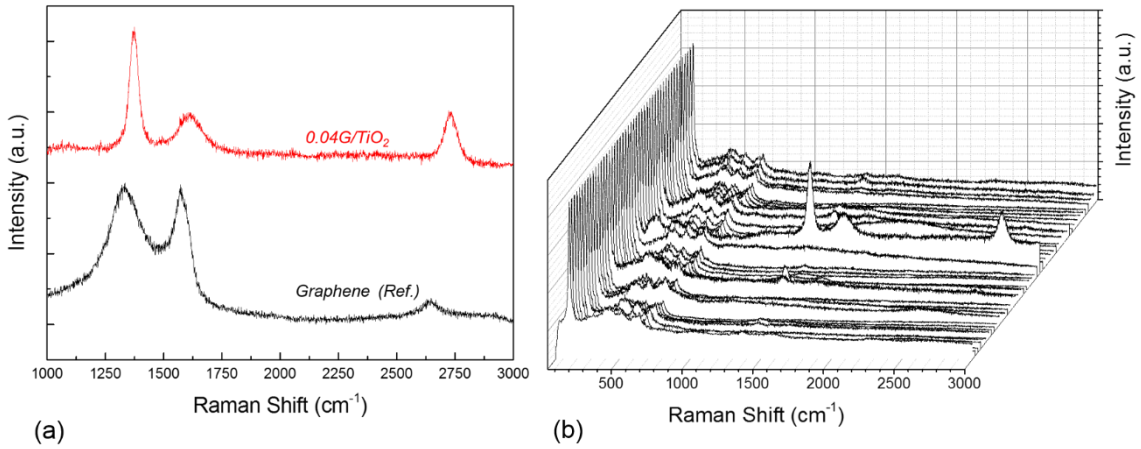

Figure S3 (a) Raman spectra showing carbon contributions of 0.04G/TiO_2 and pristine graphene (b) Raman spectra of 0.04G/TiO_2 after a mapping of 50 points

Figure S3 (a) shows the Raman spectra of the pristine graphene sample, which is compared to the carbon contributions recorded for our 0.04G/TiO_2 sample. The peaks located respectively at 1370 cm^{-1} and 1610 cm^{-1} are attributed to D and G bands of graphene whereas the 2D peak is observed around 2729 cm^{-1}.We observe a significant increase of the D band (disorder peak) with regard to pristine graphene: the intensity ratio between the D and G bands (I_D/I_G) increases up to 1.8 in the composite, whereas it is closer to 1 for the bare graphene alone. This observation is compatible with the introduction of defects by the pyrolysis process, and/or with the increase of the fraction of sp3 hybridization. This latter phenomenon could be consistent with the functionalization of graphene by the development of covalent bonds with the TiO_2 surface [1]. We also conducted Raman mapping of the 0.04G/TiO_2 annealed powder, presented in Figure S3 (b). This mapping is constituted of 50 points tested over an area of 450 μm^2 (the optical probe of our setup is around 1 μm^3). The mapping shows the good homogeneity of the sample and the large peak of anatase (at 146 cm^{-1}) is always dominant. In addition to the TiO_2 peaks, carbon contributions are observed on several measurement points and correspond to the signature of graphene.

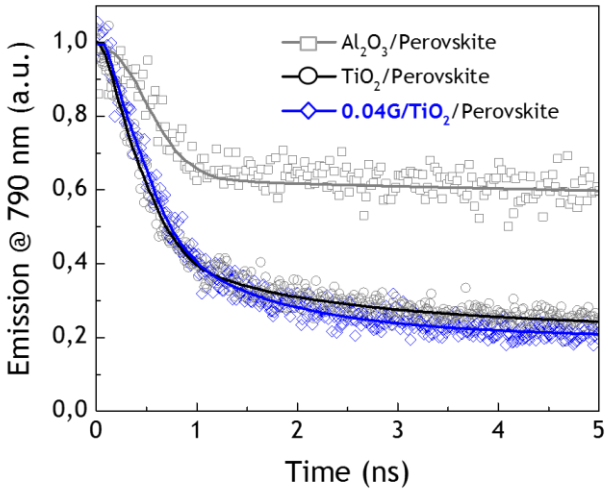

Figure S4 Transient photoluminescence (TRPL) : comparison of an electron blocking layer (Al_2O_3) and electron transport layer (TiO_2 and 0.04G/TiO_2)

Transient photoluminescence (TRPL) measurements are presented in Figure S4 and show a slightly faster PL decay kinetics in the presence of graphene compared to pure TiO_2. We note that a clear contribution of the mesoporous Al_2O_3 reference substrate is evidenced, as also reported in the literature[3].

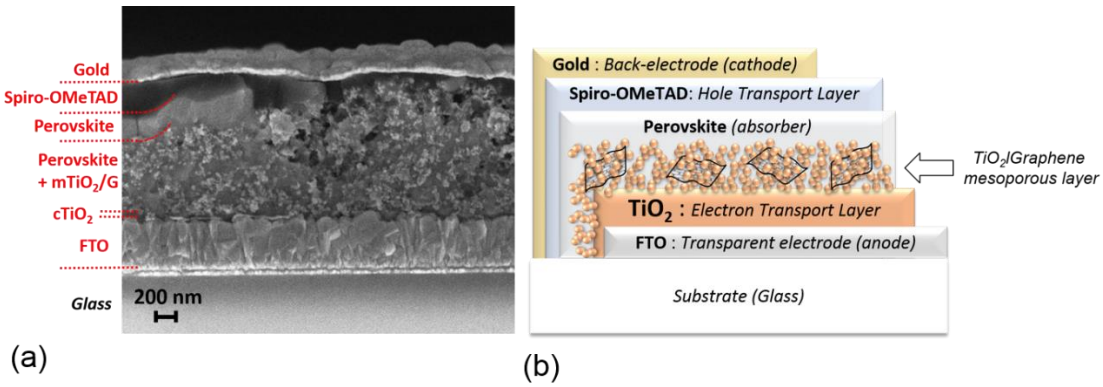

Figure S5 (a) SEM cross-section of a full perovskite solar cell (b) Perovskite solar cell architecture

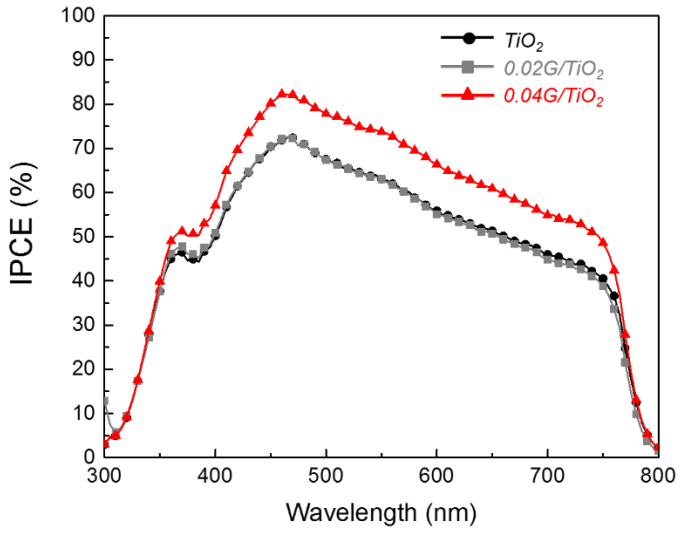

Figure S6 IPCE of perovskite solar cells with TiO_2, 0.02G/TiO_2 and 0.04G/TiO_2 based electron transport layers

Figure S6 presents typical IPCE measurements of perovskite solar cells based on TiO_2, 0.02G/TiO_2 and 0.04G/TiO_2 electron transport layers. Higher IPCE is reached for cells containing 0.04G/TiO_2, compared to the cells containing 0.02G/TiO_2 or pure TiO_2. We note that a slight decrease of the IPCE for longer wavelengths is in our case observed for all samples. This effect is associated with ion migration in the perovskite layer, which occurs over the duration of the measurement (several minutes) performed under low intensity monochromatic illumination (µW/cm²) and in short-circuit conditions, without any pre-biasing. Therefore, lower Jsc values than the ones extracted from J-V measurements under standard illumination have been estimated from IPCE curves (Jsc = 14 mA/cm² for the TiO_2-based solar cells, Jsc = 13.9 mA/cm² for 0.02G/TiO_2 and Jsc = 16.4 mA/cm² for 0.04G/TiO_2-based solar cells). Nevertheless, the general trend between samples is still observed through these measurements: a higher photo-current is obtained in case of 0.04G/TiO_2-based cells, highlighting the better charge collection efficiency upon adding of a certain fraction of graphene material in TiO_2.

Supporting information References

[1] A. Gheno, T. T. Thu Pham, C. Di Bin, J. Bouclé, B. Ratier, and S. Vedraine, “Printable WO3 electron transporting layer for perovskite solar cells: Influence on device performance and stability,” *Sol. Energy Mater. Sol. Cells*, vol. 161, pp. 347–354, 2017.

[2] V. Georgakilas *et al.*, “Functionalization of graphene: Covalent and non-covalent approaches, derivatives and applications,” *Chem. Rev.*, vol. 112, no. 11, pp. 6156–6214, 2012.

[3] V. Roiati *et al.*, “Investigating charge dynamics in halide perovskite sensitized mesostructured solar cells,” *Energy Environ. Sci.*, vol. 7, no. 6, pp. 1889–1894, 2014.